Adsorption of heavy metals and methylene blue from aqueous solution with citric acid modified peach stone

Junhua Yan[a,b], Guihong Lan[a,c], Haiyan Qiu[a **],Chao Chen[a], Yongqiang Liu[d], Guoyong Du[a], Jihong Zhang[e]*

[a] College of Chemistry and Chemical Engineering, Southwest Petroleum University, Chengdu 610500, China

[b]Sichuan Xinda Enterprise Group Co., Ltd

[c]College of Architecture and Environment, Sichuan University, 610065 Chengdu, China

[d]Faculty of Engineering and the Environment, University of Southampton, Southampton SO171BJ, United Kingdom

[e] Xinjiang oil field No. 1 gas plant

[*] Co-first author

[**]Corresponding author. E-mail:haiyanqiu316@sina.com

Abstract

Peach stones (PS) modified by citric acid (MPS) were used to remove heavy metals and methylene blue (MB) from wastewater. The effects of experimental factors such as pH, adsorbent dosage and contact time, etc were conducted. Moreover, the adsorption kinetics and isotherm studies also were investigated. According to the Langmuir isotherm model, the maximum adsorption capacities of Pb^{2+}, Cd^{2+}, Cu^{2+} and MB were 118.76, 37.48, 32.22 and 178.25 mg/g, respectively. Finally, column experiments were also carried out to investigate the adsorption of Pb^{2+} and MB. All

results indicated that peach stone has a good potential for the treatment of wastewater.

Keywords: Peach stone; Modification; Adsorption; Heavy metals; Methylene blue

1. Introduction

Environmental pollution caused by anthropogenic activities has drawn extensive attention. For example, wastewater produced from printing, leather tanning, textile and paper industries [1, 2] contains a large amount of metal ions and dyes causing serious problems to the entire biosphere, even at low concentrations. Heavy metals and dyes are toxic and have even serious detrimental effects to human through the food chain. Heavy metals are insusceptible to be biodegradable and easily accumulate in living organisms, leading to physical and mental diseases [3]. As to dyestuffs, the dyes present in wastewater can inhibit photosynthetic activity of aquatic life by preventing sunlight penetration and even can degrade into harmful compounds to threat life health[4, 5]. To minimize harm from the effluents containing heavy metals and dyes before discharging into environment, various treatment measures such as chemical precipitation, flocculation, membrane filtration, adsorption and so on have been employed to deal with them[6-8]. Among these methods, adsorption is believed to be a very promising and feasible method compared with conventional treatments due to its high efficiency and low costs. At present, a large number of adsorption materials with high adsorption capacity such as activated carbon, graphene and nanofilm have been widely researched. However, their costs of preparation and regeneration are high so that the low-cost materials are in demand.

Lignocellulosic agricultural by-products and waste materials containing a variety of functional groups such as carboxyl, hydroxyl and amine groups are abundant and cheap, which could be used to adsorb contaminants from wastewater. Considering the easy availability and low cost, great attention has been paid to use lignocellulosic wastes to remove heavy metals and dyes [9]. In recent years, various kinds of agricultural residues and by-products such as wheat bran [10], rice husk [11], wheat straw[12], soybean meal waste[13] and *Alternanthera philoxeroides*[14] have been widely investigated for wastewater treatment. However, the treatment efficiency by natural materials without any modification is not high enough for real application, so that more and more studies are being carried out to improve their adsorption capacity. To enhance the adsorption capacity of contaminants from aqueous solutions, chemical modification by HCl, NaOH, citric acid and polyethylenimine to introduce more active functional groups has been investigated [15, 16]. Nowadays, citric acid as a good modificator has been used to increase the contents of carboxyl group through esterification reaction [17]. Meanwhile, some literatures have reported that agricultural materials such as barley straw [18], corncob[19]and pine sawdust [20] modified with citric acid had excellent adsorption efficiency for heavy metals and MB.

Peach (*Prunus persica*) is a kind of popular and abundant fruit in summer in Sichuan province in China, which causes the difficulty of disposal of peach stones (PS). Because of the similar constituents of peach stone with most agricultural by-products, it is expected that PS could be employed to treat wastewater. Peach stones have been directly used as an adsorbent to adsorb lead and copper, but the adsorption capacity of

lead and copper was not high [21, 22]. Furthermore, peach stones have also been utilized as raw materials to prepare activated carbon to remove heavy metals from effluent [23, 24]. Nevertheless, the processing cost of activated carbon technology is expensive.

In this paper, PS were firstly chose as raw materials and modified by citric acid to prepare adsorbent MPS, and also were firstly used to remove heavy metals (Cd^{2+}, Cu^{2+}, Pb^{2+}) and MB from wastewater compared with literatures reported. Meanwhile, it's very helpful to realize resource recycling use and it also avoided peach PS being casually discarded. At first, the feasibility of MPS for heavy metals and MB was assessed by investigating the effects of pH, dosage, contact time, initial concentration. And to evaluate kinetic model and isotherm model, experimental data was fitted with pseudo-second order and intra-particle diffusion kinetic models, the Langmuir isotherm model and Fredunlich isotherm model, respectively. Moreover, metal binding mechanisms by MPS was investigated by being characterized with elemental analyzer, Fourier transformed infrared spectroscopy (FTIR), scanning electron microscopy (SEM), surface area analyzer and thermogravimetric analysis (TGA). Finally, column experiments were investigated to stimulate the adsorption of Pb^{2+} and MB.

2. Materials and Methods

2.1. Materials

Peach stones were obtained from Longquan district, Chengdu, China. Citric acid (CA), copper nitrate, cadmium nitrate, lead nitrate, sodium hydroxide and methylene blue (MB) were purchased from Kelong chemical reagent factory (Chengdu, China).

All reagents were of analytical grade and deionized water was used in all experiments. And all experiments were carried out three times.

2.2. Preparation of adsorbent MPS

2.2.1. Chemical modifications of peach stones with critic acid

Peach stones were firstly washed by deionized water to remove dust and other impurities, and dried in an oven for 24 h at 90℃. Then these dried peach stones were milled and sieved to obtain 50-60 mesh fractions (labeled as PS). To increase the proportion of active surfaces and to inhibit tannin compounds [20], twenty grams of sieved peach stones were soaked in 400 ml of 0.1 M NaOH and stirred in a magnetic stirrer for 1 h at room temperature. Then the soaked peach stones were rinsed several times with deionized water to remove excess base until the pH reached approximately to neutral, dried overnight at 50℃ in the oven (labeled as BPS) and stored in plastic bags for the following experiments.

Modification experiment of peach stones with critic acid was carried out according to the literatures reported in previous years [25, 26]. Firstly, the dry samples (BPS) were mixed with 0.8 M CA (optimum concentration) in a ratio of 1.0 g base-peach stones to 12.5 ml CA and stirred in a magnetic stirrer for 2 h at 300 rmp at room temperature. Next, the samples were poured into a stainless steel tray and dried at 50℃ in an oven for 24 h. Afterward, the dry samples were reacted for 4 h (optimum time) at 120℃ (optimum temperature) in an oven. The modification conditions were optimized by varying concentrations of critic acid (0.2-1 M), reaction times (1-5 h) and reaction

temperature (100-150℃). Finally, the products were soaked in deionized water for 1h and washed repeatedly until there was no turbidity when 10 ml of 0.1 M lead nitrate was added. The final reaction products were dried overnight in an oven at 50℃ (labeled as MPS).

2.2.2. Carboxyl determination

A dry sample (0.2 g) was slurried in water and 0.1 M NaOH was added. After being stirred for 24 h, the mixture was back-titrated with 0.1 M HCl to the phenolphthalein end point. Meanwhile, conversion factors were determined using citric acid as standards. PS was used as a control.

2.3. Adsorbent characterization

The C, H and N contents of the materials before and after modification were obtained by a CHN Elemental Analyzer (Var10EL-III, Germany). The changes of functional groups on the materials before and after modification and adsorption of heavy metals and MB were determined by FTIR spectrometer (WQF520, China). Surface morphology of the samples was characterized using scanning electron microscopy (SEM, JSM-7500F) at 10.0 kV. Surface areas of the samples were analyzed by surface area analyzer (ST-MP-9, US) using Brunauer-Emmett-Teller (BET) method. Thermal gravity analysis (TGA) of the materials before and after modification were determined using a TG instrument (NETZSCH STA 449F3) under air atmosphere scanned from 40 to 800℃.

2.4. Preparation of different heavy metal and MB solutions

Copper nitrate, cadmium nitrate, lead nitrate and MB were dissolved in deionized water to attain stock solutions of 1000 mg/L Cu^{2+}, Cd^{2+}, Pb^{2+} and MB and then diluted to different initial concentrations according to the experimental requirements. The solutions containing heavy metal ions before and after adsorption were determined by flame atomic absorption spectrophotometry (FAAS, AA-7020, Beijing, China). MB was analyzed by UV-Vis spectrophotometer (V-1800, Mapada) at the maximum wavelength (665 nm), and the standard curve of MB was fitted according to the experimental data and was shown in Fig.1.

Fig. 1 Standard curve of MB

2.5. Adsorption studies

All adsorption experiments were conducted by adding 0.2 g MPS into 50 ml 200 mg/L solutions containing Cu^{2+}, Pb^{2+}, Cd^{2+} and MB respectively at 30 ± 2℃ and shaken at 250 rpm on a constant temperature shaker (QYC-200, Chengdu, China). The solution pH was adjusted by 0.1 M HCl and 0.1 M NaOH. And the samples were collected at suitable time intervals for 300 min. Then the solutions containing Cu^{2+}, Pb^{2+} and Cd^{2+} were determined by FAAS. The concentrations of MB solutions were determined by UV-Vis spectrophotometer.

The adsorption capacity (q_e mg/g) and removal rate (w %) were calculated according to the following equations,

$$q_e = \frac{(C_0 - C_e)V}{m} \qquad (1)$$

$$w = \frac{C_0 - C_e}{C_0} \times 100\% \qquad (2)$$

Where q_e and w are the uptake amount (mg/g) and the removal rate (%) at equilibrium, respectively. C_0 and C_e are the initial and equilibrium concentrations of heavy metals and MB (mg/L), respectively. m is the mass of adsorbent.

2.5.1. Effect of adsorbent dosage

The effects of adsorbent dosage on the adsorption capacity of Cu^{2+}, Pb^{2+}, Cd^{2+} and MB were investigated by adding different amounts of MPS (0.05, 0.1, 0.2, 0.3, 0.4 and 0.5 g) to 50 ml 200 mg/L solutions containing different heavy metals and MB, respectively. After adsorption, the solutions were withdrawn to analyze their concentrations according to section 2.4.

2.5.2. Effect of initial pH

Batch experiments were carried out in the pH ranges of 2-7 to investigate the influence of pH on adsorption of Cu^{2+}, Pb^{2+}, Cd^{2+} and MB. The pH was adjusted by 0.1 M HCl and 0.1 M NaOH.

2.5.3. Adsorption kinetic studies

To investigate adsorption kinetics of MPS on heavy metals and MB, adsorption experiments were performed by mixing 0.6 g MPS with 150 ml 200 mg/L solution containing Cu^{2+}, Pb^{2+}, Cd^{2+} and MB respectively. Samples were withdrawn at different time intervals ranging from 10 to 300 min and the concentrations of solution were analyzed according to section 2.4.

2.5.4. Adsorption isotherm studies

Adsorption isotherms were carried out by adding 0.2 g MPS into 50 ml solution containing Cu^{2+}, Pb^{2+}, Cd^{2+} and MB respectively with different concentrations varying from 50 to 1000 mg/L. And the solutions before and after adsorption by MPS were determined by the above-mentioned methods.

2.6. Column adsorption studies

Column experiments of Pb^{2+} and MB were performed in a glass column with 0.4 cm internal diameter and 15.0 cm length. MPS were packed with the bed height of 5.0 cm, 6.0 cm and 7.0 cm, respectively. The initial concentrations of Pb^{2+} and MB were 200 mg/L diluted by the stock solutions of 1000 mg/l of Pb^{2+} and MB, respectively. The pH values of Pb^{2+} and MB were 5.0 and 6.0 adjusted by 0.1M HCl and 0.1M NaOH, respectively. And the solutions were pumped up-flow through the fix-bed column at a flow rate of 3.8 ml/min. Samples were collected at various time intervals and the concentrations of samples were analyzed according to section 2.4.

3. Results and Discussion

3.1. Effects of experimental conditions on modification

In order to determine the optimum concentration of critic acid, reaction time and temperature, batch modification experiments were carried out at various concentrations of CA (0.2-1 M), reaction time (1-5 h) and reaction temperature (100-150℃). The final samples were determined by estimating the carboxyl contents to obtain the optimum modification conditions. The modification mechanism was illustrated in Fig. 2.

Fig. 2 Esterification reaction of peach stone cellulose and critic acid

The carboxyl contents at different concentrations of critic acid, reaction time and temperature are summarized in Table 1. As shown in Table 1 (a), the carboxyl contents increased with the increase of concentrations of critic acid and reached the maximum at 0.8 M, and then decreased. In Table 1 (b) and Table 1 (c), with the increase of reaction time and temperature, the carboxyl contents reached the maximum at 4 h and 120℃, respectively. Consequently, 0.8 M critic acid, 4 h and 120℃ were chosen as the optimum modification condition with 0.00544 mol/g free carboxyl groups on MPS. All samples were prepared at the optimum conditions for the next adsorption experiments.

Table 1 Effect of the concentration of citric acid, reaction time and temperature on citric acid (CA) and peach stone (PS) reaction.

3.2. Adsorbent characterization

3.2.1. Elemental analyses of PS and MPS

As known, PS are mainly composed of cellulose, hemicelluloses and lignin so that it’s feasible for modifying PS by CA. The hydroxyl groups on PS reacted with CA by forming an ester linkage to introduce carboxyl groups. The results of elemental analysis of PS before and after modification by CA are summarized in Table 2. As indicated in Table 2, the carbon and hydrogen percentage of MPS reduced comparing with PS. Nevertheless, the oxygen percentage and molar ratio of O/C of MPS were higher than PS, which proved the success of modification by critic acid.

Table 2 The elemental analysis results of PS and MP

3.2.2. Thermogravimetric analysis of PS and MPS

The TG curves of PS and MPS are presented in Fig. 3. According to the results of TG curves of PS and MPS in Fig. 3, it can be seen that the process of mass loss for PS and MPS was composed of three stage, including dehydration, active pyrolysis and passive pyrolysis. As shown in Fig. 3, the first stage of the mass loss of PS and MPS was ranged from 42 to 210℃ and 42 to 188℃ respectively, attributing to the loss of free water and bound water. At the second stage, the temperature range of PS was 210 to 340℃, which can be associated with the active pyrolysis of cellulose and hemicelluloses. From Fig. 3, it can be clearly observed that the beginning of temperature of MPS was lower and the temperature range was wider than PS ascribed to the successful chemical modification by CA. Meanwhile, the third stage of the mass loss of PS ranged from 340 to 518℃ which can be attributed to the further pyrolysis of cellulose[27]. Comparing with PS, the temperature range of MPS at the third stage was wider than PS from 348 to 573℃ due to the further decomposition of the carboxyl groups introduced and cellulose. Moreover, the lignin pyrolysis of PS and MPS existed the whole process [28].

Fig. 3 TG curves of PS and MPS

3.2.3. Surface morphology and BET surface area analysis

As shown in Fig. 4, the SEM micrographs of PS before and after the chemical modification by CA were investigated. From Fig. 4a, it can be seen that the microtopography of PS was irregular and porous. In comparing to the micrograph of

PS, the surface structures of BPS and MPS did not change obviously and the porous structure still existed. This indicated that modification did not change the porous structure of PS, which still can play an important role in adsorption of contaminants.

Fig. 4 SEM micrographs of PS (a), BPS (b) and MPS (c)

The BET surface area and pore volume of PS and MPS were listed in Table 3. In comparison with PS, the BET surface area of MPS significantly decreased from 0.330 to 0.0296 m^2/g, which could be ascribed to the change of the pore distribution after the modification by critic acid. It's clear that the pore volume was low about 3.675 dm^3/g for PS, however the pore volume of MPS was lower about 2.710 dm^3/g. It could be explicated that some large pores were clogged by CA during the chemical modification. Therefore, the results indicated that the adsorption capacity of heavy metals and dyes can be improved due to the introduction of carboxyl groups and the presence of porous structure.

Table 3 The BET surface area and pore volume of PS and MPS

3.3.3. Fourier transform infrared spectroscopy analysis

The FTIR spectra of PS before and after modification and all MPS samples after the adsorption of heavy metals and MB are shown in Fig. 5. Based on the contents of PS mainly containing cellulose, hemicellulose and lignin, it's obvious that a large of groups (carboxyl, hydroxyl, ether and so on) could be observed from FTIR spectra.

As indicated in Fig. 5, the spectrum of PS showed a strong and broad peak around 3441cm^{-1} attributed to the existence of OH groups. The peak appeared at 2907 cm^{-1} was

ascribed to the CH stretching band. The characteristic stretching vibration adsorption band observed at 1745 cm^{-1} was assigned to the carboxyl groups in hemicellulose. The band around 1515 cm^{-1} was the amide group. The adsorption peak for 1254 cm^{-1} was due to the syringyl ring and CO stretching in lignin and xylan (hemicellulose) and the band around 1039 cm^{-1} was the characteristic of the COC and OH groups of primary hydroxyl stretching in cellulose and hemicellulose [9, 20]. In comparison with FTIR spectrum of PS, it can be seen that the intensity of the peak of carboxyl group obviously increased after the chemical modification of PS by CA. The strong stretching band of carboxyl group located at 1738 cm^{-1} was attributed to the esterification reaction by citric acid [29]. In addition, after the modification of PS by CA, the stretching vibration bands of OH shifted from 3441 cm^{-1} to 3431 cm^{-1} and obviously broadened, but the peak at 2907 cm^{-1} changed little, the peak of amide group at 1515 cm^{-1} became sharp, the peak around 1254 cm^{-1} disappeared, and hydroxyl groups shifted from 1039 cm^{-1} to 1031 cm^{-1}.

After the completion of adsorption of heavy metals and MB by MPS, it can be seen that the FTIR spectra obviously changed comparing with MPS. From Fig. 5, the OH stretching bands around 3441cm^{-1} of all samples loaded by heavy metals and MB shifted little and broadened, which were ascribed to the formation of hydrogen bonds between the hydroxyl groups on MPS and heavy metals or MB. The intensity of the peaks at 1738 cm^{-1} and 1515 cm^{-1} decreased especially for MPS loaded by heavy metals. It can be assigned to the chelation between carboxyl or amide groups on MPS and heavy metals or MB. However, the peak decrease of MPS loaded by MB was slight comparing

with heavy metals onto MPS. The results can be elaborated by the different adsorption mechanism between heavy metals and MB. Meanwhile, it's obvious that the peak at 1031 cm^{-1} of MPS decreased after adsorption indicating that the COC and OH groups participated in the adsorption reaction of heavy metals and MB. The intensity of the band of MPS loaded by MB located at 1031 cm^{-1} decreased. Moreover, the peaks of MPS loaded by heavy metals shifted slightly and the corresponding peak intensity also weakened comparing with MPS. The peak for MPS-Cd^{2+} loaded was 1023 cm^{-1}, 1039 cm^{-1} for MPS-Cu^{2+} and 1016 cm^{-1} for MPS-Pb^{2+}.

Fig. 5 FTIR spectra of PS, MPS and MPS after adsorption of heavy metals and MB (MB-MPS: MPS after adsorption of MB, Cd-MPS: MPS after adsorption of Cd, Cu-MPS: MPS after adsorption of Cu, Pb-MPS: MPS after adsorption of Pb)

3.3. Effect of pH on heavy metals and MB adsorption

The solution pH has a significant effect on adsorption capacity in the adsorption process. Fig. 6 shows the change trends of Cd, Cu, Pb and MB with the increase of pH. As shown in Fig. 6, the uptake amounts of Cd, Cu, Pb and MB was low at low pH, which attributed to strong competition adsorption between adsorbates and hydrogen ions and electrostatic repulsion from the surface of adsorbent. However, it can be seen that all adsorption capacities increased with the increasing pH due to the reducing concentration of H^+, the increasing electrostatic attractions and ion-exchange.

It's well known that the heavy metal species present in aqueous solution and the surface charge of adsorbent can be significantly affected by pH [9]. At low pH, there existed strong electrostatic repulsion due to the positive charge of adsorbent and strong

competition between H^+ and heavy metals. With the increase of pH, the positive charge on the adsorbent surface started to decrease and charged negatively resulting in the adsorption capacity increasing. However, when the solution pH containing heavy metal ions reached a certain value, it's easy to form precipitation. According to the literature reported, when the pH value is over 5.8, the precipitation of $Cu(OH)_2$ and $Pb(OH)_2$ start to form[30]. As for Cd, the $Cd(OH)_2$ precipitation exist at pH 7 [19]. Therefore, to avoid the precipitation playing a major role, the next adsorption experiments of Cu and Pb were investigated at pH 5, and Cd was at pH 6. With regard to MB, MB in solution was positively charged. At pH < 4, the uptake capacity was low due to the strong competition between H^+ and active sites on MB. At pH > 4, it can been seen that the adsorption amounts increased and remained stable after pH 6, attributed to electrostatic attraction. So pH 6 was selected to study the adsorption of MB at next experiments.

Fig. 6 Effect of solution pH on heavy metals and MB adsorption onto MPS (initial concentration : 200 mg/L; dosage: 0.2 g; 30°C; contact time: 2 h)

3.4. Effects of adsorbent dosage

The effects of different adsorbent dosage from 1 to 10 g/L on the removal rates of Cu, Cd, Pb and MB by MPS are shown in Fig. 7. It can be seen from Fig. 7a the all adsorption rates increased with the increase of adsorption dosage. It can be ascribed to more active sites and greater surface area provided with the increasing amount of adsorbent. Fig. 7b shows that the adsorption capacities of heavy metals and MB decreased with the increase of adsorbent dosage, which can be due to un-saturation of

adsorption sites that were conductive to the decrease of adsorption uptake [31].

Fig. 7 Effect of adsorbent dosages on heavy metals and MB onto MPS (initial concentration : 200 mg/L; pH: Cu, Pb-5, Cd, MB-6; 30℃; contact time: 2 h)

3.5. Adsorption kinetics

Fig. 8 illustrates the effects of contact time on adsorption capacity of heavy metals and MB. As shown in Fig. 8a, the adsorption process was consisted of two stages: a rapid adsorption stage over a few time due to explosion of more adsorption sites and a slower adsorption stage until the equilibrium state reached attributed to the saturation of active sites. From Fig. 8a, it's clear that heavy metals and MB were rapid to reach the adsorption equilibrium. Therefore, 180 min was suitable to be chosen as contact time for the further experiments.

In order to better understand the adsorption kinetics of heavy metals and MB by MPS, the experiment data were fitted with pseudo-second-order and intra-particle diffusion models. The pseudo-second-order kinetic model [32] is expressed as:

$$\frac{t}{q_t} = \frac{1}{k\, q_e^2} + \frac{t}{q_e} \qquad (3)$$

The intra-particle diffusion model [33] is given as follows:

$$q_t = k_p t^{0.5} + C \qquad (4)$$

Where q_e (mg/g) and q_t (mg/g) are the adsorption uptake of heavy metals and MB by MPS at equilibrium and at time t, respectively. k ($g.mg^{-1}. min^{-1}$) is the pseudo-

second-order rate constant calculated from the plots of t/q_t against t, and k_p (mg. $h^{0.5}$. g^{-1}) is the intra-particle diffusion rate constant gained from the slope of straight-line portions of the plots of q_t against $t^{0.5}$, and C is a constant obtained from the intercept of gained from the plots.

As shown in Fig. 8b, it's obvious that the experiment data can be fitted with pseudo-second-order kinetic models well. The regression coefficients (R^2) data listed in Table 4 were high, about 0.9996, 0.9983, 0.9843 and 0.9991 for MB, Cd, Cu and Pb respectively. Meanwhile, the calculated q_e values of heavy metals and MB were in agreement with the experimental data. Therefore, it indicated that the chemical adsorption could be the rate limiting step in the heavy metals and MB adsorption process[4].

In Fig. 8c, it can be clearly seen that the intra-particle diffusion models were consisted of two straight lines, which confirmed that the intra-particle diffusion contained two steps: the liner step with a rapid adsorption process assigned to the external surface adsorption or boundary layer diffusion, and the intra-particle diffusion step [5]. Nevertheless, the liner plots in Fig. 8c did not pass through the origin indicating that the intra-particle diffusion were not the rate controlling step.

Table 4 Kinetic parameters for MB, Cd, Cu, Pb adsorption on M-PS

Fig. 8 Effect of contact time on heavy metals and MB (a), the pseudo-second-order kinetic model (b) and intra-particle diffusion plots (c) on heavy metals and MB adsorption by MPS (initial concentration: 200 mg/L; dosage: 0.2 g; pH: Cu, Pb-5, Cd, MB-6; 30°C)

3.6. Adsorption isotherms

Batch experiments were carried out for investigating the effects of initial concentrations on adsorption of heavy metals and MB by MPS. As depicted in Fig. 9a, the amounts of heavy metals and MB adsorption quickly increased with the increase of adsorbent dosage and then slowly increased until the equilibrium gradually reached. At low concentrations, the increasing uptakes of heavy metals and MB were ascribed to the sufficient active sites on the adsorbent. Furthermore, the increasing initial concentrations of heavy metals and MB were conducive to form strong driving force to overcome mass transfer resistance in adsorption process. However, at the high concentration, more heavy metals and MB were left un-adsorbed due to the the saturation of binding sites of MPS so that the capacities increased slowly and almost kept stable.

To evaluate the adsorption capacities of heavy metals and MB by M-PS and illustrate the characterization of adsorption process, Langmuir and Freundlich models were employed in this study. Langmuir isotherm assumes a monolayer adsorption over a homogeneous adsorbent surface and each molecule adsorbed onto the surface [16]. Langmuir isotherm model [34] can be expressed as follows:

$$\frac{C_e}{q_e} = \frac{C_e}{q_{\max}} + \frac{1}{q_{\max} K_L} \qquad (5)$$

Where q_e and C_e are the equilibrium adsorption capacity (mg/g) and equilibrium concentration (mg/L), respectively. $q_{\max}$ is the maximum adsorption capacity (mg/g), and K_L is the Langmuir constant (L/mg).

Freundlich model [35, 36] which is still an empirical equation used to simulate the multilayer adsorption is represented as follows:

$$\log q_e = \log k_f + \frac{1}{n}\log C_e \qquad (6)$$

Where q_e and C_e are the equilibrium concentration (mg/L) and equilibrium adsorption capacity (mg/g), respectively. k_f and n are the Freundlich constant. The Langmuir and Freundlich constants of the adsorption of heavy metals and MB were calculated from the slopes and intercepts of the plots of C_e/q_e versus C_e (Fig. 9b) and $\log q_e$ versus C_e (Fig. 9c) and summarized in Table 5.

As illuminated in Fig. 9 and Table 5, the results indicated that the adsorption process of Cd, Cu and Pb can be fitted with Langmuir isotherm model well with high regression coefficients ($R^2 > 0.9$). In addition, the experimental data of Pb and Cu can be fitted with Freundlich model indicating that the adsorption process of Pb and Cu might be governed by multiple mechanisms. Regarding to MB, the adsorption process was more suitable for being described by Freundlich isotherm model ($R^2 = 0.9244$) than Langmuir isotherm model ($R^2 = 0.8705$), indicating that the adsorption process of MB can be multilayer adsorption. For the adsorption of heavy metals, the maximum uptakes evaluated by Langmuir isotherm followed the order: Pb>> Cd> Cu, and were 118.76, 37.48 and 32.22 mg/g, respectively. In the case of MB, the maximum adsorption capacity was 178.25 mg/g. These results also further proved that MPS was a promising adsorbent to treatment effluent containing heavy metals and dyes.

Table 5 Parameters of Langmuir and Freundlich isotherm

Fig. 9 Effect of initial concentration on heavy metals and MB (a), Langmuir isotherm model (b) and Freudlich isotherm model (c) on heavy metals and MB adsorption by MPS (dosage: 0.2 g; pH: Cu, Pb-5, Cd, MB-6; 30℃; contact time: 2 h)

3.6. Column studies

To study the practical application of MPS, the column experiments were conducted to investigate the adsorption of Pb^{2+} and MB. The breakthrough curves of MPS were presented in Fig. 10. As shown in Fig. 10, it can be seen that the breakthrough times of Pb^{2+} and MB increased with the increase of bed height. Since more time was spent to pass through the column with the higher bed height, Pb^{2+} and MB had longer contact time with MPS leading to higher capacity.

Fig. 10 Breakthrough curves of Pb^{2+} and MB with different bed heights (bed height: 5 cm, 6 cm, 7 cm; initial concentration: 200 mg/L; room temperature; pH: Pb-5, MB-6; flow rate: 3.8 ml/min)

4. Conclusions

In this paper, peach stones modified by citric acid as a new adsorbent were studied to remove heavy metals and MB from wastewater. Batch adsorption experiments showed that pH, adsorbent dosage, contact time and initial concentration have significant effects on the adsorption of heavy metals and MB. Kinetics studies indicated that the experimental data of heavy metals and MB can be fitted with pseudo-second order model well. Therefore, the chemical adsorption was the rate-limiting step for the adsorption of heavy metals and MB. Isotherm studies suggested that heavy metals can be fitted with the Langmuir isotherm well and Pb can be fitted with Freundlich, but MB

followed Freundlich isotherm model well. Furthermore, column experiments of Pb^{2+} and MB also were conducted. The results indicated that Pb^{2+} and MB have high adsorption capacity. All results confirm that MPS has a potential for the removal of heavy metals and MB. And it also realized the regeneration use of PS well and avoided the waste of resources.

Acknowledgements

This work was supported by China Postdoctoral Science Foundation (Grant No. 2015M572477) and the Opening Project (YQKF201406) of Oil & Gas Applied Chemistry Key Laboratory of Sichuan Province.

References

1. Adamczuk, A.;& Kołodyńska, D. (2015). Equilibrium, thermodynamic and kinetic studies on removal of chromium, copper, zinc and arsenic from aqueous solutions onto fly ash coated by chitosan. Chemical Engineering Journal, 274, 200.

2. Zhang, W.; Li, H.; Kan, X.; Lei, D.; Han, Y.; Jiang, Z.;Yang, Hu.; Li, A.; Cheng, R. (2012). Adsorption of anionic dyes from aqueous solutions using chemically modified straw. Bioresource Technology, 117(10), 40.

3. Zhou, Y.; Zhang, R.; Gu, X.; Lu, J.(2015) Adsorption of divalent heavy metal ions from aqueous solution by citric acid modified pine sawdust. Separation Science and Technology, 50(2), 245.

4. Liu, F.; Zou, H.; Hu, J.; Liu, H.; Peng, J.; Chen, Y.; Lu, F; Huo Y. (2016) Fast removal of methylene blue from aqueous solution using porous soy protein isolate based composite

beads. Chemical Engineering Journal, 287, 410.

5. Mahmoud, D. K.; Salleh, M. A. M.; Wan, A. W. A. K.; Idris, A.; Abidin, Z. Z. (2012) Batch adsorption of basic dye using acid treated kenaf fibre char: equilibrium, kinetic and thermodynamic studies. Chemical Engineering Journal, s 181-182(2), 449.

6. Zeng, G.; He, Y.; Zhan, Y.; Zhang, L.; Pan, Y.; Zhang, C.; Yu, Z. (2016) Novel polyvinylidene fluoride nanofiltration membrane blended with functionalized halloysite nanotubes for dye and heavy metal ions removal. Journal of Hazardous Materials, 317, 60.

7. Sajab, M. S.; Chia, C. H.; Zakaria, S.; Jani, S. M.; Ayob, M. K.; Chee, K. L. (2011) Citric acid modified kenaf core fibres for removal of methylene blue from aqueous solution. Bioresource Technology, 102(15), 7237

8. Mata, Y. N.; Blázquez, M. L.; Ballester, A.; González, F.; Muñoz, J. A. (2009) Biosorption of cadmium, lead and copper with calcium alginate xerogels and immobilized fucus vesiculosus. Journal of Hazardous Materials, 163(s 2-3), 555.

9. Al-Ghouti, M. A.; Li, J.; Salamh, Y.; Al-Laqtah, N.; Walker, G.; Ahmad, M. N. (2010) Adsorption mechanisms of removing heavy metals and dyes from aqueous solution using date pits solid adsorbent. Journal of Hazardous Materials, 176(1-3), 510.

10. Kaya, K.; Pehlivan, E.; Schmidt, C.; Bahadir, M. (2014) Use of modified wheat bran for the removal of chromium(VI) from aqueous solutions. Food Chemistry, 158(8), 112.

11. Krishnani, K. K.; Meng, X.; Christodoulatos, C.; Boddu, V. M. (2008) Biosorption mechanism of nine different heavy metals onto biomatrix from rice husk. Journal of Hazardous

Materials, 153(3), 1222.

12. Li, Y.; Zhao, B.; Zhang, L.; Han, R. (2013) Biosorption of copper ion by natural and modified wheat straw in fixed-bed column, Desalination and Water Treatment, 51, 5735.

13. Witek-Krowiak, A.; Harikishore, K. R. D. (2013) Removal of microelemental Cr(III) and Cu(II) by using soybean meal waste--unusual isotherms and insights of binding mechanism. Bioresource Technology, 127(127C), 350.

14. Wang, X. S.; Qin, Y. (2006) Removal of Ni(II), Zn(II) and Cr(VI) from aqueous solution by alternanthera philoxeroides biomass. Journal of Hazardous Materials, 138(3), 582.

15. Velazquezjimenez, L. H.; Pavlick, A.; Rangelmendez, J. R. (2013) Chemical characterization of raw and treated agave bagasse and its potential as adsorbent of metal cations from water. Industrial Crops & Products, 43(1), 200.

16. Sajab, M. S.; Chia, C. H.; Zakaria, S.; Khiew, P. S. (2013) Cationic and anionic modifications of oil palm empty fruit bunch fibers for the removal of dyes from aqueous solutions. Bioresource Technology,128C(1), 571.

17. Low, K. S.; Lee, C. K.; Mak, S. M. (2004) Sorption of copper and lead by citric acid modified wood. Wood Science and Technology, 38(8), 629.

18. Pehlivan, E.; Altun, T.; Parlayici, S. (2013) Modified barley straw as a potential biosorbent for removal of copper ions from aqueous solution. Food Chemistry, 135(4), 2229.

19. Leyva-Ramos, R., Landin-Rodriguez L. E., Leyva-Ramos S. & Medellin-Castillo N. A. 2012 Modification of corncob with citric acid to enhance its capacity for adsorbing cadmium(ii) from

water solution. Chemical Engineering Journal, 180(3), 113.

20. Zhang, R.; Zhou, Y.; Gu, X.; Lu, J. (2015) Competitive adsorption of Methylene Blue and Cu2+ onto citric acid modified pine sawdust. CLEAN-Soil, Air, Water, 43(1), 96.

21. Rashed, M. N. (2006) Fruit stones from industrial waste for the removal of lead ions from polluted water. Environmental Monitoring & Assessment, 119(1-3), 31.

22. Hansen H. K., Arancibia F. & Gutiérrez C. 2010 Adsorption of copper onto agriculture waste materials. Journal of Hazardous Materials,180(1-3), 442.

23. Ntuli, V.; Hapazari, I. (2012) Sustainable waste management by production of activated carbon from agroforestry residues. South African Journal of Science, 109(1-2), 1.

24. Girgis, B.S.; Elkady, A. A.; Attia, A.A.; Fathy, N.A. M. A A.W. (2009) Impact of Air Convection on H3PO4-Activated Biomass, Carbon Letters, 10 (2), 114.

25. Marshall, W. E., Wartell, L. H., Boler D. E., Johns M. M. & Toles C. A. 1999 Enhanced metal adsorption by soybean hulls modified with citric acid. Bioresource Technology, 69(69), 263-268.

26. Wing, R. E. 1996 Corn fiber citrate: preparation and ion-exchange properties. Industrial Crops & Products, 5(4), 301-305.

27. Rayón, E.; Ferrandiz, S.; Rico, M. I.; López, J.; Arrieta, M. P. (2014) Microstructure, mechanical, and thermogravimetric characterization of cellulosic by-products obtained from biomass seeds. International Journal of Food Properties, 18(6), 1211.

28. Yang, H.; Yan, R.; Chen, H.; Dong, H. L.; Zheng, C. (2007) Characteristics of hemicellulose, cellulose and lignin pyrolysis. Fuel,86(12-13), 1781.

29. Zhu, B.; Fan, T.; Zhang, D. (2008) Adsorption of copper ions from aqueous solution by citric acid modified soybean straw. Journal of Hazardous Materials, 153(1-2), 300.

30. Wang, H.; Gao, B.; Wang, S.; Fang, J.; Xue, Y.; Yang, K. (2015) Removal of Pb(II), Cu(II), and Cd(II) from aqueous solutions by biochar derived from KMnO4 treated hickory wood. Bioresource Technology, 197, 356.

31. Gong, J. L.; Wang, X. Y.; Zeng, G. M.; Chen, L.; Deng, J. H.; Zhang, X. R.; Niu, Q. (2012) Copper (II) removal by pectin-iron oxide magnetic nanocomposite adsorbent. Chemical Engineering Journal, 185-186(1), 100.

32. Pitsari, S.; Tsoufakis, E.; Loizidou, M. (2013) Enhanced lead adsorption by unbleached newspaper pulp modified with citric acid. Chemical Engineering Journal, 223(3), 18.

33. Fan, H. L.; Li, L.; Zhou, S. F.; Liu, Y. Z. (2016) Continuous preparation of Fe3O4 nanoparticles combined with surface modification by L-cysteine and their application in heavy metal adsorption. Ceramics International, 42(3), 4228.

34. Badruddoza A. Z; Tay, A. S.; Tan, P. Y.; Hidajat, K.; Uddin, M. S. (2010) Carboxymethyl-β-cyclodextrin conjugated magnetic nanoparticles as nano-adsorbents for removal of copper ions: synthesis and adsorption studies. Journal of Hazardous Materials, 185(2-3), 1177.

35. Chakravarty, S.; Pimple, S.; Chaturvedi, H. T.; Singh, S.; Gupta, K. K. (2008) Removal of copper from aqueous solution using newspaper pulp as an adsorbent. Journal of Hazardous Materials, 159(2-3), 396.

36. Qiu, H.; Yan, J.; Lan, G.; Liu, Y.; Song, X.; Peng, W.; Cui, Y. (2016). Removal of Cu2+ from

wastewater by modified xanthan gum (xg) with ethylenediamine (eda). Rsc Advances, 6.

Figure captions:

Fig. 1 Standard curve of MB

Fig. 2 Esterification reaction of peach stone cellulose and critic acid

Fig. 3 TG curves of PS and MPS

Fig. 4 SEM micrographs of PS (a), BPS (b) and MPS (c)

Fig. 5 FTIR spectra of PS, MPS and MPS after adsorption of heavy metals and MB (MB-MPS: MPS after adsorption of MB, Cd-MPS: MPS after adsorption of Cd, Cu-MPS: MPS after adsorption of Cu, Pb-MPS: MPS after adsorption of Pb)

Fig. 6 Effect of solution pH on heavy metals and MB adsorption onto MPS (initial concentration : 200 mg/L; dosage: 0.2 g; 30□; contact time: 180 min)

Fig. 7 Effect of adsorbent dosages on heavy metals and MB onto MPS (initial concentration : 200 mg/L; pH: Cu, Pb-5, Cd, MB-6; 30□; contact time: 180 min)

Fig. 8 Effect of contact time on heavy metals and MB (a), the pseudo-second-order kinetic model (b) and intra-particle diffusion plots (c) on heavy metals and MB adsorption by MPS.

Fig. 9 Effect of initial concentration on heavy metals and MB (a), Langmuir isotherm model (b) and Freudlich isotherm model (c) on heavy metals and MB adsorption by MPS.

Fig. 10 Breakthrough curves of Pb^{2+} and MB with different bed heights (bed height: 5 cm, 6 cm, 7 cm; initial concentration: 200 mg/L; room temperature; pH: Pb-5, MB-6; flow rate: 3.8 ml/min)

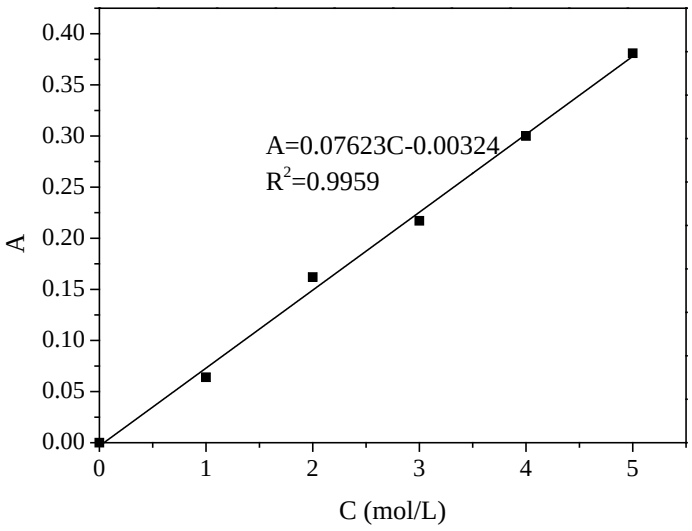

Fig. 1 Standard curve of MB

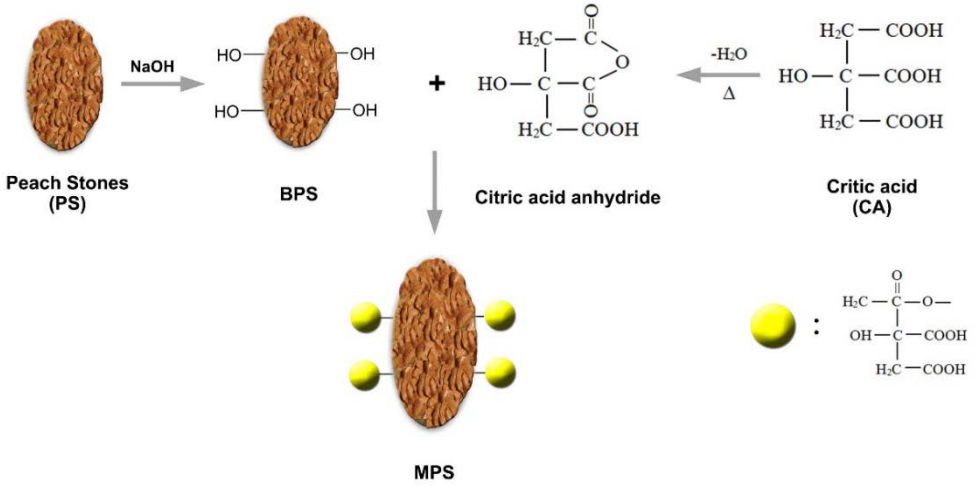

Fig. 2 Esterification reaction of peach stone cellulose and critic acid

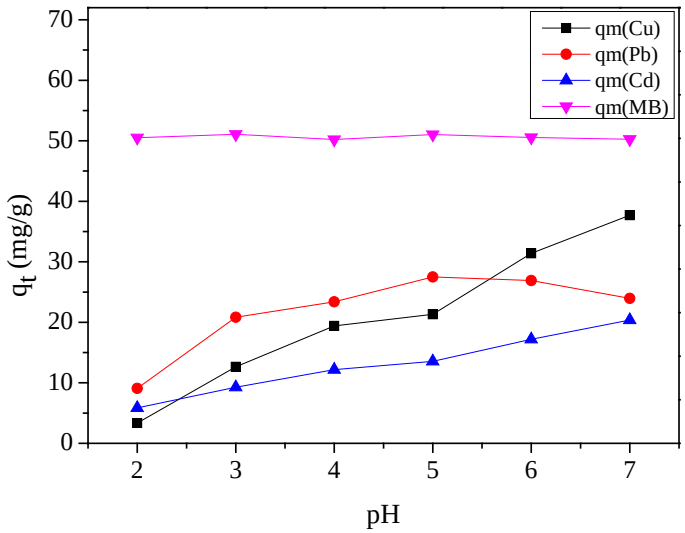

Fig. 3 TG curves of PS and MPS

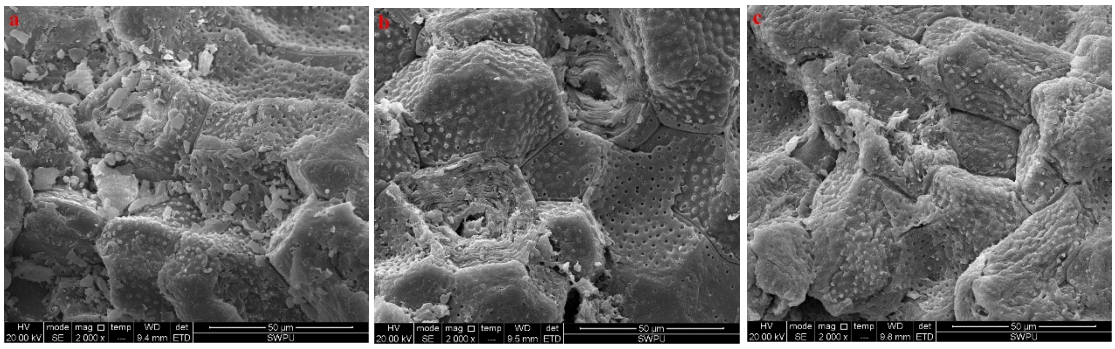

Fig. 4 SEM micrographs of PS (a), BPS (b) and MPS (c)

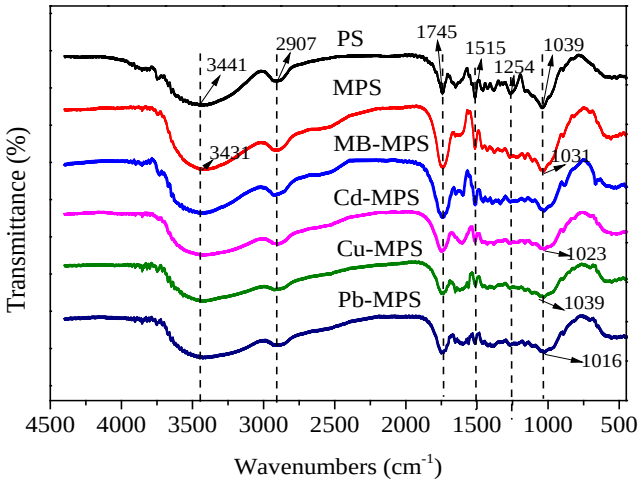

Fig. 5 FTIR spectra of PS, MPS and MPS after adsorption of heavy metals and MB.

(MB-MPS: MPS after adsorption of MB, Cd-MPS: MPS after adsorption of Cd, Cu-MPS: MPS after adsorption of Cu, Pb-MPS: MPS after adsorption of Pb)

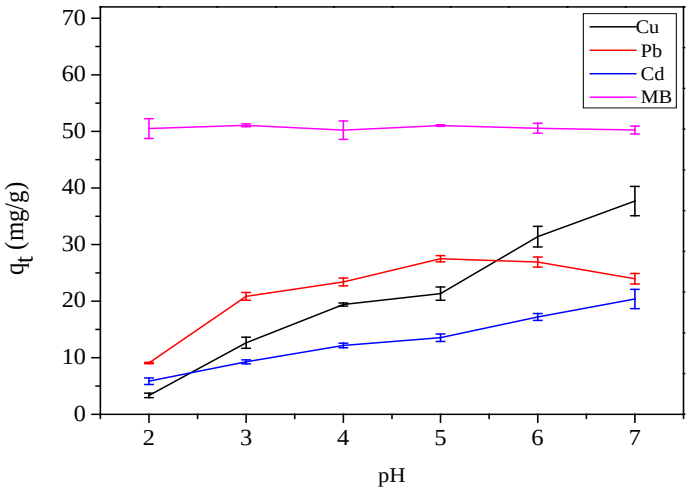

Fig. 6 Effect of solution pH on heavy metals and MB adsorption onto MPS (initial concentration : 200 mg/L; dosage: 0.2 g; 30℃; contact time: 180 min)

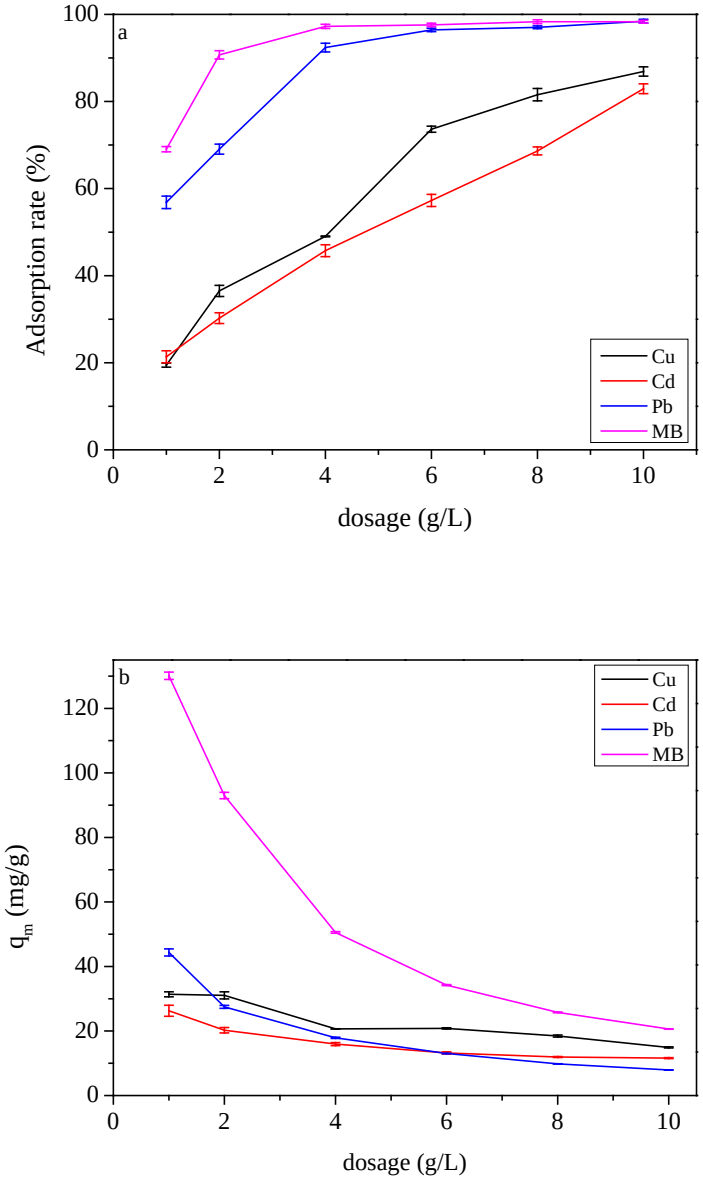

Fig. 7 Effect of adsorbent dosages on heavy metals and MB onto MPS (initial concentration : 200 mg/L; pH: Cu, Pb-5, Cd, MB-6; 30℃; contact time: 180 min)

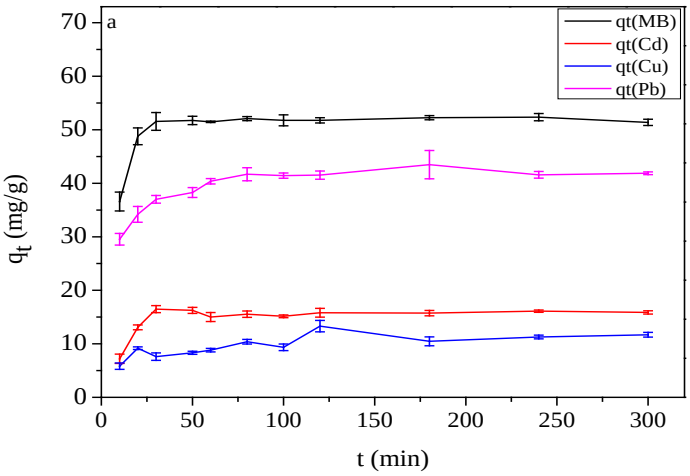

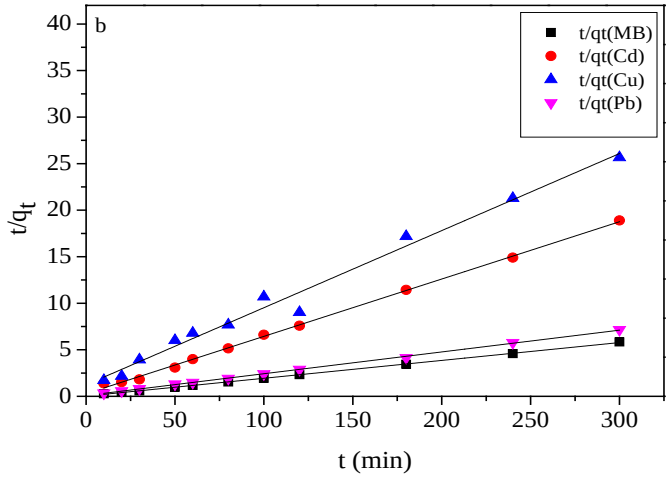

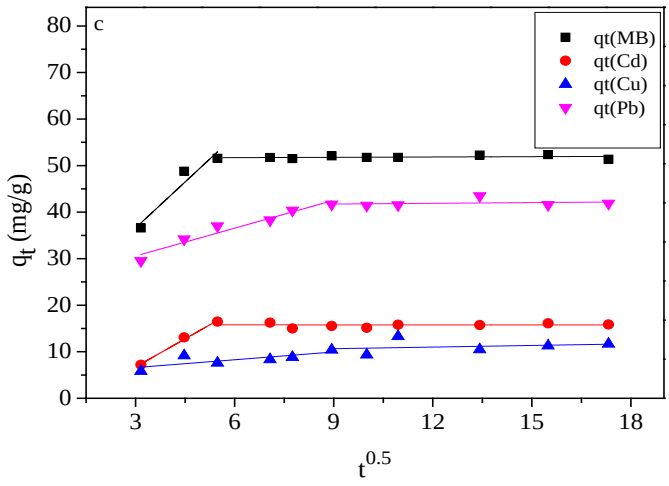

Fig. 8 Effect of contact time on heavy metals and MB (a), the pseudo-second-order kinetic

model (b) and intra-particle diffusion plots (c) on heavy metals and MB adsorption by MPS.

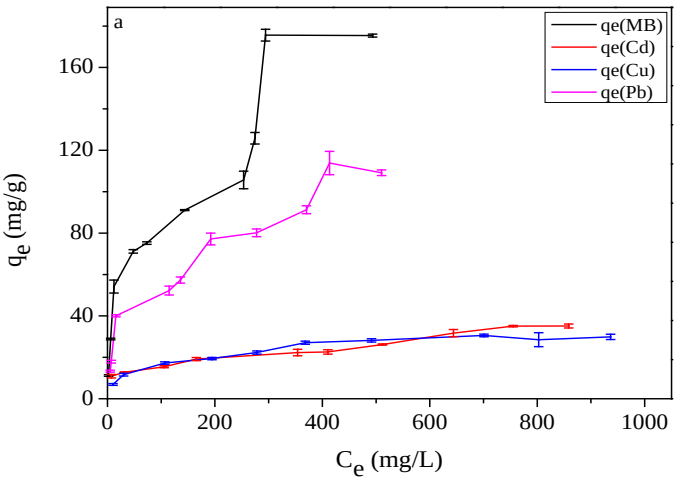

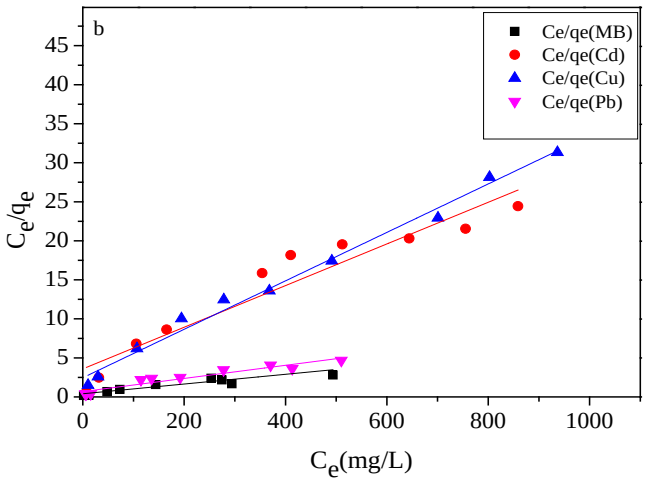

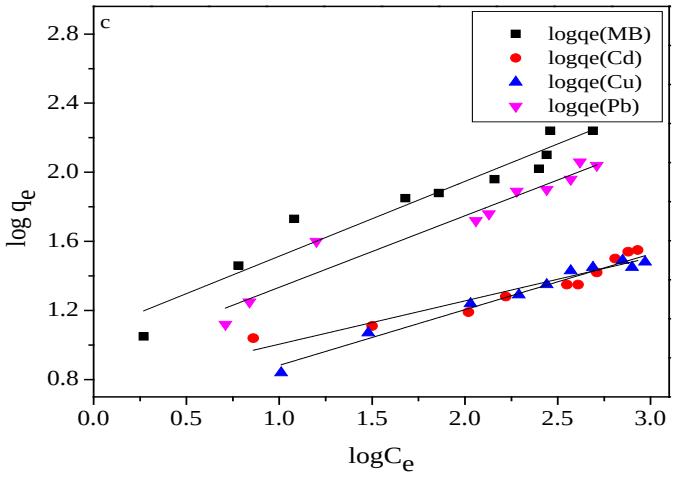

Fig. 9 Effect of initial concentration on heavy metals and MB (a), Langmuir isotherm model (b) and Freudlich isotherm model (c) on heavy metals and MB adsorption by MPS.

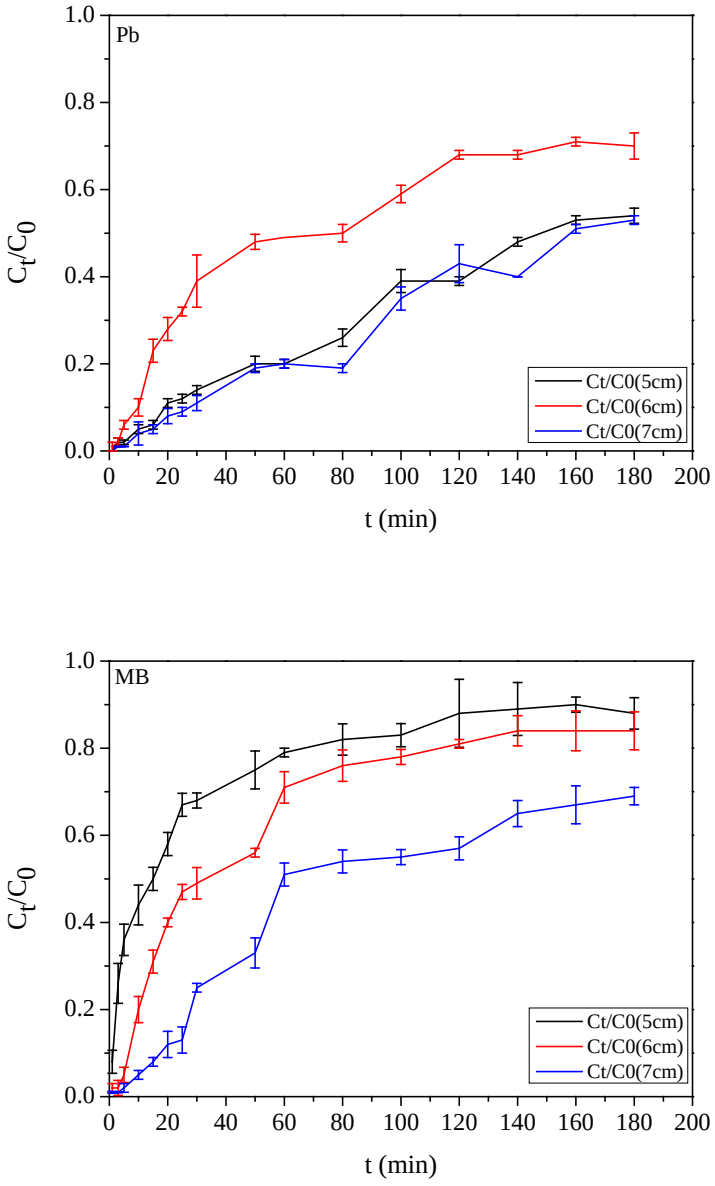

Fig. 10 Breakthrough curves of Pb^{2+} and MB with different bed heights (bed height: 5 cm, 6 cm, 7 cm; initial concentration: 200 mg/L; room temperature; pH: Pb-5, MB-6; flow rate: 3.8 ml/min)

Table captions:

Table 1 Effect of the concentration of citric acid, reaction time and temperature on citric acid (CA) and peach stone (PS) reaction.

Table 2 The elemental analysis results of PS and MPS

Table 3 The BET surface area and pore volume of PS and MPS

Table 4 Kinetic parameters for MB, Cd, Cu, Pb adsorption on M-PS

Table 5 Parameters of Langmuir and Freundlich isotherm

Table 1 Effect of the concentration of citric acid, reaction time and temperature on citric acid (CA) and peach stone (PS) reaction.

(a)

Adsorbent	Reaction time (h)	Reaction temperature (℃)	CA concentration (mol/L)	COOH (mol/g)
PS	-	-	-	0.000589
MPS			0.2	0.00184
MPS			0.4	0.00242
MPS	4	120	0.6	0.00386
MPS			0.8	0.00521
MPS			1	0.00505

(b)

Adsorbent	Reaction time (h)	Reaction temperature (℃)	CA concentration (mol/L)	COOH (mol/g)
MPS	1			0.00356
MPS	1.5			0.00386
MPS	2	120	0.8	0.00461

MPS	3			0.00449
MPS	4			0.00544
MPS	6			0.00527

(c)

Adsorbent	Reaction time (h)	Reaction temperature (℃)	CA concentration (mol/L)	COOH (mol/g)
MPS		100		0.00477
MPS		110		0.00469
MPS	4	120	0.8	0.00544
MPS		130		0.00406
MPS		140		0.00398
MPS		150		0.00277

Table 2 The elemental analysis results of PS and MPS

	C (%)	O (%)	H (%)	N (%)	O/C (mol/mol)
PS	48.13	45.64	6.201	0.031	0.7112
MPS	47.51	46.80	5.677	0.014	0.7388

Table 3 The BET surface area and pore volume of PS and MPS

	BET surface area (m^2/g)	pore volume (dm^3/g)
PS	0.330	3.675
MPS	0.0296	2.710

Table 4 Kinetic parameters for MB, Cd, Cu, Pb adsorption on M-PS

	MB	Cd	Cu	Pb
Pseudo-second-order kinetic model				
k (g. mg^{-1}. min^{-1})	0.0003683	0.003792	0.006864	0.0005474
q_e (mg/g)	52.11	16.24	12.07	42.74
R^2	0.9996	0.9983	0.9843	0.9991
intra-particle diffusion kinetic model				
k_p (mg. h$^{0.5}$. g^{-1})	6.591	4.024	0.5592	1.995
C	16.84	-5.330	4.924	24.59
R^2	0.8540	0.9877	0.5102	0.9325

Table 5 Parameters of Langmuir and Freundlich isotherm

	MB	Cd	Cu	Pb
Langmuir model				
q_{max} (mg. g^{-1})	178.25	37.48	32.22	118.76
K_f (L/mg)	69.84	136.1	79.10	81.41
R^2	0.8705	0.9133	0.9893	0.9161
Freundlich model				
K_f (mg/g)	12.05	5.682	31.83	8.321
n	2.309	3.990	17.83	2.415
R^2	0.9244	0.8961	0.9728	0.9367